

# FATIGUE CRACK INITIATION AND PROPAGATION AT HIGH TEMPERATURE IN A SOFTENING MARTENSITIC STEEL

B. Fournier<sup>1,2</sup>, M. Sauzay<sup>1</sup>, M. Mottot<sup>1</sup>, V. Rabeau<sup>1</sup>, A. Bougault<sup>1</sup>, A. Pineau<sup>2</sup>

<sup>1</sup>CEA, DEN-DMN-SRMA, Bâtiment 455, 91191 Gif-sur-Yvette cedex, France.

<sup>2</sup>ENSMP, Centre des Matériaux P.-M. Fourt, UMR CNRS 7633, BP 87, 91003 Evry, France.  
benjamin.fournier@cea.fr

## ABSTRACT

Fatigue and creep-fatigue tests were conducted in air at 823K on a modified 9Cr-1Mo martensitic steel. The usual cyclic softening behaviour of this steel is firstly depicted and two main testing parameters (the cumulated viscoplastic strain and the cyclic strain amplitude  $\Delta\epsilon_i$ ) are found to be relevant in the description of its evolution. The relation between the number of cycles to failure of pure fatigue tests and the cyclic strain amplitude is then expressed. Moreover the deleterious effect of cyclic creep strains and particularly of compressive ones is highlighted. The fatigue lifetime reduction due to hold periods is all the more pronounced as the cyclic strain amplitude is low. Finally a series of microscopic observations points out the major influence of oxidation phenomena on both the crack initiation and propagation. On this basis an explanation of the more damaging effect of compressive holds is expressed in terms of damage interaction between mechanical loading and environmental effects.

## Introduction

The martensitic steels of the 9-12%Cr family are used for many various applications in the energy industry [1-3]. The modified 9Cr-1Mo steel is a candidate for several components of the generation IV nuclear reactors. Typical in-service conditions require operating temperatures between 673 and 873 K, which means that the creep behaviour of these steels is of primary interest. In addition, the repeated start- and stop-operations during service lead to loadings of creep-fatigue type, with very long hold times (typically one month). As complete tests with such long hold periods cannot, of course, be conducted in laboratory, the actual in-service mechanical behaviour must be extrapolated from the results of short term mechanical tests.

This article presents the results of such fatigue and creep-fatigue mechanical tests with a specific emphasis on the cracking phenomena. The results of the mechanical tests are firstly presented in terms of cyclic behaviour and fatigue lifetime. Secondly a series of microscopic observations of the surface, the fracture surface and polished cross-sections of the specimens are presented and compared. On these basis the main damage phenomena are finally discussed in comparison to those considered in the usual damage accumulation codes.

## Material and experiments

The experiments were conducted using a T-91 steel produced by Usinor (Arcelor, France). The chemical composition is given in Table 1. The steel sheet was austenitized at 1323K for 30 min, quenched and tempered at 1053K for 1h. At 823K the tensile properties are  $R_{e0.2\%} = 310\text{MPa}$  and  $R_m = 370\text{MPa}$ . The as-tempered martensitic microstructure presented in figure 1 is very fine and presents several scales [4,5]. The thinnest microstructural scale consists in subgrains with diameter close to  $0.7\mu\text{m}$ . The mechanical tests were carried out in air at 823K. Low cycle fatigue (LCF) tests were conducted on MAYES ESM100 servo-mechanical machines with resistance furnace heating. The axial strain was measured by a capacitive extensometer directly fixed on the calibrated part. The accuracy of this device is better than  $0.5\mu\text{m}$  that allows to conduct LCF tests with a strain amplitude as small as 0.1%. The LCF tests were conducted under total strain control conditions. A symmetrical triangular wave form signal with an axial strain rate of about  $2 \cdot 10^{-3} \text{ s}^{-1}$  was used for the cyclic part of the tests. In addition to the pure LCF tests, a series of creep-fatigue tests was conducted, in order to study the interaction between creep and fatigue loadings. For these hold time tests, the stress was held constant at tensile (or compressive) peak stress as depicted in figure 2.a. Thanks to a numerical system, the tensile and compressive stress peaks were recorded for all cycles. Figure 2.b presents the evolution of these two peak stresses in addition to those of the mean stress and the stress range. As a general feature, LCF tests with hold times induce a mean stress of sign opposite to those of the dwell period. Indeed, when the peak stress is held constant, a creep strain is added to the cyclic strain amplitude ( $\Delta\epsilon_i$ ). This additive strain must be compensated during the stress reversal, which induces an increased opposite peak stress. Practically speaking in the particular case of the tensile hold time test presented in figure 2.b, an almost constant compressive mean stress ( $-50\text{MPa}$ ) exists.

**Table 1 – Chemical composition of the T-91 steel under study (Arcelor).**

Element	C	N	Cr	Mo	Mn	Si	Nb	V
Wt(%)	0.088	0.043	8.776	0.915	0.354	0.329	0.078	0.191

## Results and discussion

### Mechanical behaviour :

As it can be noticed in figure 2.b, the modified 9Cr-1Mo steel softens under cyclic loading. This softening effect largely reported in the literature [5,7,8] can be, at least partly, correlated to the microstructural coarsening and to the decrease of the dislocation density occurring during fatigue and creep-fatigue loadings [9,14,47]. In a previous work [10], two relevant testing parameters were identified to describe this softening effect. These are on the one hand the cumulated plastic strain and on the other hand the strain amplitude per cycle ( $\Delta\epsilon_t$ ) which governs the number of activated slip systems). As shown in figure 3.a, the higher the strain amplitude per cycle is, the stronger and the quicker the softening effect is. These two testing parameters were taken into account in the micromechanical modelling based on a boundary annihilation mechanism proposed in [9-10] and gave encouraging results in the prediction of the cyclic behaviour of martensitic steels.

This softening effect is also illustrated in figure 3.b where the monotonic tensile curve is compared to the cyclic stress-strain curve obtained under pure fatigue loading and creep-fatigue loading (with a creep strain per cycle equals to 0.1% and 0.5%). While a visible increasing difference between the monotonic and cyclic stress is observed, the addition of a creep strain at each cycle does not seem to lower the consolidation curve obtained at  $N_f/2$  (where  $N_f$  is the number of cycles to failure). This figure suggests that, the “saturated” states obtained for tests at different cyclic creep strains may correspond to comparable microstructures.

### Fatigue and Creep-Fatigue lifetimes :

The relation between fatigue lifetime and the total strain per cycle is plotted in figure 4.a. As the strain amplitude decreases, the fatigue lifetime and its scatter increase. A usual analysis of the cyclic endurance is given by the Langer description :

$$\epsilon_t = \epsilon_0 + A.N_f^B \quad (1)$$

The corresponding parameters of this relation fitted with an acceptable accuracy on the pure fatigue endurance data are given in table 2.

**Table 2 - Value of the parameters of the Langer's equation**

$\epsilon_0(\%)$	A	B
0.31	107.8	-0.67

Figure 4.a also presents the tensile hold creep-fatigue endurance data. It can be noticed that these creep-fatigue lifetimes are strongly reduced compared to the pure fatigue ones, at a given strain amplitude. For a given cyclic strain amplitude ( $\Delta\epsilon_t$ ), the larger the added creep strain, the shorter the fatigue lifetime as noticed in figure 4.b. This tendency is all the more evident as the strain amplitude decreases (e.g. at  $\Delta\epsilon_t = 0.4\%$  a creep strain of 0.1% reduces the fatigue lifetime up to 71%, while for  $\Delta\epsilon_t = 1\%$  the lifetime is reduced of 34%). This deleterious effect of hold periods seems to depend of course on the material but also on the testing conditions (atmosphere, temperature,...) since, for example, in the case of a 12%Cr steel in a humid environment the addition of a dwell time tends on the contrary to increase the fatigue lifetime [11].

Nevertheless, if the lifetimes between tensile and compressive creep-fatigue tests are compared, the compressive hold appears more damaging since at all tested strain levels, the fatigue lifetime was shorter with respect to the corresponding tensile hold test. This general feature which is more pronounced for low strain amplitudes is illustrated by figure 4.b. Such a deleterious effect of compressive holds with respect to tensile holds has already been reported in several studies dedicated to 9%Cr steels [12-16]. However, for other materials (2.25%Cr [17] or 1%CrMoV [18] steels for example) the more damaging effect of compressive hold has not been observed. Actually, as creep damage accumulation (e.g. grain boundary cavitation) occurs under tensile hold, the opposite result (tensile hold more damaging than compressive hold) is to be expected when usual creep-fatigue damage phenomena are considered.

Dealing with creep-fatigue interactions, three usual types of damage are considered [19] : slip-induced grain boundary cracking, oxidation damage, creep cavitation. The following observations try to identify which kind of damage was predominant in the present testing conditions.

#### Microscopic observations :

Figures 5, 6 and 7 present three observations of the sample surfaces, fracture surfaces and ground cross-sections of samples loaded respectively in pure-fatigue ( $\Delta\epsilon_t=0.7\%$ ), creep-fatigue with tensile hold time ( $\Delta\epsilon_t=0.4\%$ ,  $\epsilon_{creep}=0.1\%$ ), creep-fatigue with compressive hold time ( $\Delta\epsilon_t=0.4\%$ ,  $\epsilon_{creep}=0.1\%$ ). In all cases the tests were conducted in air at 823K.

The observations of the fracture surfaces were made with the oxide layer etched away. Both the tensile hold creep-fatigue specimens and the pure fatigue specimen show a low number of secondary cracks visible on the free surface, contrary to the compressive hold case where a high density of large and wide secondary cracks is visible.

In all cases the fracture surfaces show a mainly transgranular propagation (striations were observed) of the main crack (as also noticed in [8,20]). Under creep-fatigue loadings the early stages of propagation seem to indicate a mixed mode propagation (trans and intergranular). The most striking difference lays again in the number of cracks. Indeed, in the case of pure fatigue and tensile creep-fatigue, a single main crack propagated and led to fracture, whereas for the compressive creep-fatigue test the fracture surface reveals that nine large cracks propagated and contributed to the final fracture.

No usual creep cavities were observed on cross sections, whatever the loading condition studied. As presented in figures 5 and 6, samples submitted to tensile creep-fatigue and pure fatigue loadings present highly branched and bifurcated cracks, while in figure 7 the widely opened straight cracks of the compressive creep-fatigue sample are visible. The same branched shape of the cracks were observed [8] under pure fatigue loading. However, for longer hold times, higher strain levels and fatigue relaxation tests (1h at  $\Delta\epsilon_t=0.5\%$ ) typical crack shapes for tensile and compressive holds were found to be opposite to the present observations (wide and straight for tensile hold times and branched for compressive ones) [12].

Another interesting result coming from the observation of the cross-sections is related to the interaction with environment. Under static oxidation, the usual oxide layer formed on modified 9Cr-1Mo steels under various atmospheres is duplex, consisting of an external layer of an Fe-rich oxide (hematite or magnetite) and of an inner layer of a Cr-rich spinel [21-25]. In the present case, all the observed cracks (initiated under fatigue and creep-fatigue loadings) present an oxide layer all along their lips (the wide straight cracks of the compressive hold specimen being completely filled with oxide). This means that the propagation of the cracks are influenced by the interaction with environment.

#### Interactions between mechanical loadings and environment :

Evidence of the influence of the environment on the crack initiation has also been found. The higher crack density observed under creep-fatigue loadings with compressive hold is thought to be related directly to the mechanical behaviour of the oxide layer. Indeed several studies [16,17] showed that the main part of the fatigue lifetime under vacuum was linked to the crack initiation stage for high cycles fatigue. Additionally under compressive hold conditions, the usual duplex oxide layer observed under static oxidation (and for the other mechanical loadings), is replaced by a multilayered morphology, as shown in figure 9. This multilayered oxide comes from the successive cracking followed by accelerated oxidation steps, as described in the literature [14-16,31,32]. This oxide cracking process leads to the formation of a thicker and highly damaged (figure 9) oxide layer and promotes the initiation of cracks in the substrate (due to the stress concentration at the oxide crack tip). This process does not occur for all loading conditions tested, which can be attested by the oxide thicknesses measured on the tested samples. Figure 10 shows the comparison between the oxide thicknesses measured under static oxidation in air at 823K and the thicknesses measured after various mechanical tests. The two multilayered oxide scales correspond to the largest oxide thicknesses.

In the case of the two creep fatigue tests observed in figure 6 and 7, only the compressive hold one presents this multilayered morphology resulting from the successive cracking of the oxide scale. To try to explain it, one must first notice that, as the oxide scale will mainly grow during the hold period, it means that for compressive hold times this oxide layer will mainly form at the most compressive stress. Thus during almost the whole fatigue cycle, the oxide scale will be loaded in tension as schematically represented in figure 11. Several cracking mechanisms are discussed in the literature either on empirical or theoretical bases [33-44]; they seem to indicate that cracking in tension occurs for lower applied strains than in compression which may explain why the compressive hold specimen presents this multilayered oxide scale. The numerous cracks on the compressive hold sample substrate are thus supposed to initiate on the oxide layer cracks.

Figure 10 also shows that the multilayered morphology was observed for a tension hold test, but at a higher applied strain. Nevertheless, even though both the tensile and the compressive hold tests induce oxide cracks initiation, the number of cycles to failure was found to be slightly lower in the compressive hold case. This might be due to the fact that for the compressive hold sample (the oxide layer is thus mainly submitted to tension) the oxide preferentially fails by cracking through its thickness, inducing stress concentration in the substrate. Whereas in the tension hold case (the oxide layer is thus mainly submitted to compression), the oxide tends to spall or buckle which accelerates the apparent oxidation rate but may induce no cracking in the substrate. Additionally, in the compressive hold case, a mean tensile stress exists (figure 2b) and may also explain the reduced fatigue lifetime.

As far as the crack propagation is concerned, various types of mechanisms can result from the oxidation of the material, several of which being mentioned by King and Cotterill [26] (adsorption phenomena leading to slip irreversibility, alloy rewelding in the compression stage inhibited by the oxide layer...). In the case of 9%Cr steels, tests in both air and vacuum conditions showed that the oxidation increases the crack propagation rate [26-29]. Nevertheless, a crack completely filled with oxide as shown in figure 7 may stop to propagate. Additionally, when the oxide layer is not completely adherent to the substrate, a layer of internal oxidation [30] is observed as shown in figure 8. This internal oxidation occurs preferentially along laths boundaries where Cr-rich precipitates lay. This form of oxidation, when it take place at the crack tip (figure 8.b) and increases the crack propagation rate.

#### Identification of the main damage mechanisms :

The previous observations showed that, for all the creep levels tested, no usual creep cavitation damage as been observed at 823K. Nevertheless, at higher temperatures (close to 873K), a usual creep-fatigue interaction (intergranular damage, creep cavities, ...) was observed in several studies [5,16] and a single evidence of very small intergranular cavities is reported at 823K [12]. This may question the applicability of the various calculation methods of the cumulated creep and fatigue damage [5,12,18,45,46] for these short creep or relaxation times at 823K.

Additionally the present observations and a lot of experimental evidences from the literature seem to indicate a strong influence of the interactions between mechanical loading and environment. Indeed, it was shown that the propagation of the fatigue cracks is accelerated by the oxide layer forming on the crack lips and by the damaging effect of the internal oxidation observed. Moreover, the oxide layer cracking induced during some tests comes from the mechanical loadings. These oxide cracks favour then the initiation of cracks in the substrate, which strongly reduces the number of cycles necessary to initiate a macroscopic fatigue crack. Thus, the effect of environment was found to play a major role both in the initiation and propagation stages, whereas these environmental effects are often not taken into account in usual damage accumulation codes.

### **Conclusions**

A series of pure fatigue and creep fatigue tests was conducted in air at 823K on a modified 9Cr-1Mo martensitic steel. The usual cyclic softening behaviour of this steel was highlighted and appeared to depend both on the cumulated applied viscoplastic strain and on the cyclic strain range ( $\Delta\epsilon_t$ ).

The number of cycles to failure was found to correctly follow the Langer description for the pure fatigue loadings. The fatigue lifetime was found to decrease for increasing applied creep strain and compressive hold periods revealed themselves more damaging than tensile ones. These deleterious effects are all the more pronounced as the fatigue applied strain is low.

In order to identify the main damage mechanisms occurring in these tests, extensive microscopic observations were realized. No creep cavitation damage has been observed, whatever the testing conditions applied. On the contrary a major influence of the oxidation was highlighted on both the initiation and the propagation of fatigue cracks. These interactions between mechanical loadings and environment enable to explain, at least partially, the reduced fatigue lifetime associated to compressive hold periods.

These results show that, at 823K, in air and for the creep levels tested, the two main damage mechanisms are fatigue and oxidation, which may question the applicability of the usual damage accumulation strategies that often hardly take into account the influence of environment and its interactions with mechanical loadings.

### **Acknowledgments**

The Direction of Nuclear Energy of the CEA is acknowledged for financial support through the DDIN/SF project.

### **References**

1. R.W. Swindeman, M.L. Santella, P.J. Maziasz, B.W. Roberts, K. Coleman. Issues in replacing Cr-Mo steels and stainless steels with 9Cr-1Mo-V steel. Pressure Vessels and Piping 81, 507-512, 2004.
2. Creep & Fracture in high temperature components – Design & Life assessment issues. Proceedings of the ECCC Creep Conference, sept, 2005 London UK, Destech Publications, Inc.
3. P.J. Ennis, W.J. Quadackers. 9-12% Chromium steels: application limits and potential for further development. Parsons 2000 advanced materials for 21<sup>st</sup> century turbines and power plant. Proceedings of the fifth international charles parsons turbine conference p265-275.
4. J. M. Marder, A. R. Marder, Trans. ASME 62 (1969) 1.
5. B.G. Gieseke, C.R. Brinkman, P.J. Maziasz. The influence of thermal aging on the microstructure and fatigue properties of modified 9Cr-1Mo steel. Microstructures and mechanical properties of aging material. 1993.
6. M. Sauzay, M. Mottot, L. Allais, M. Noblecourt, I. Monnet, J. Périnet, Nucl. Eng. Des. 232 (2004) 219-236.
7. Kunz, P. Lukas. Cyclic stress-strain behavior of 9Cr-1Mo steel at positive mean stress. Materials science & engineering A319-321, 555-558, 2001.
8. A. Nagesha , M. Valsan, R. Kannan, K. Bhanu Sankara Rao, S.L. Mannan. Influence of temperature on the low cycle fatigue behaviour of a modified 9Cr-1Mo ferritic steel. International Journal of fatigue 24, 1285-1293, 2002

9. M. Sauzay, H. Brillet, I. Monnet, M. Mottot, F. Barcelo, B. Fournier; A. Pineau. Cyclically induced softening due to low-angle boundary annihilation in a martensitic steel. *Materials Science and Engineering A*, 400-401, 241-244, 2005.
10. B. Fournier, M. Sauzay, M. Mottot, H. Brillet, I. Monnet, A. Pineau. Experimentally based modelling of cyclically induced softening in a martensitic steel at high temperature. ECCC creep conference, Creep & Fracture in high temperature components - Design & life assessment issues. London UK, Destech Publications, Inc. 2005.
11. K.M. Perkins, M.R. Bache. Corrosion fatigue of a 12%Cr low pressure turbine blade steel in simulated service environments. *International Journal of fatigue*, 2005.
12. K. Aoto, R. Komine, F. Ueno, H. Kawasaki, Y. Wada. Creep-fatigue evaluation of normalized and tempered modified 9Cr-1Mo. *Nuclear Engineering and Design* 153 97-110. 1994.
13. R.L. Hecht, J.R. Weertman. The effect of environment on High-Temperature hold time fatigue behaviour of annealed 2.25 pct Cr 1 pct Mo steel. *Metallurgical and materials transactions* 29A, 2137-2145, 1998.
14. S. Kim, J.R. Weertman. Investigation of microstructural changes in a ferritic steel caused by high temperature fatigue. *Metallurgical Transactions* 19A, 999-1007, 1988.
15. R.L. Hecht, J.R. Weertman. Periodic oxide cracking on Fe2.25Cr1Mo produced by high temperature fatigue tests with a compression hold. *Metallurgical Transactions* 24A, 327-333, 1993.
16. R. L. Hecht. Mechanisms operating during high-temperature fatigue with hold periods in two chromium ferritic steels. PhD dissertation, Northwestern University, 1992.
17. B.A. Kschinka, J.F. Stubbins. Creep-fatigue-environment interaction in a bainitic 2.25wt.%Cr-1wt.%Mo steel forging. *Mat. Sci. & Eng. A* 110, 89-102, 1989.
18. S.R. Holdsworth. Creep-fatigue properties of high temperature turbine steels. *Materials at high temperature*, 18(4) , 261-265, 2001.
19. A. Pineau. Mechanisms of creep-fatigue interactions. *Advances in Fatigue Science and Technology*, 283-311, 1989.
20. J. Aktaa, M. Lerch. Fatigue crack growth in EUROFER 97 at different temperatures. Final report, Tasks : TW1-TTMS-002, D22 and TW-TTMS-002a, D22. 2005.
21. A.P. Greeff, C.W. Louw, H.C. Swart. The oxidation of industrial FeCrMo steel. *Corrosion Science* 42, 1725-1740, 2000.
22. A.S. Khanna, P. Rodriguez and J.B. Gnanamoorthy. Oxidation kinetics, breakaway oxidation, and inversion phenomenon in 9Cr-1Mo steels. *Oxidation of Metals*, Vol.26, N°3/4, 1986.
23. C. Ostwald, H.J. Grabke. Initial oxidation and chromium diffusion. I. Effects of surface working on 9-20% Cr steels. *Corrosion Science*, 46, 1113-1127, 2004.
24. W.M. Stobbs, S.B. Newcomb, E. Metcalfe. A Microstructural study of the oxidation of Fe-Ni-Cr alloys. II 'Non-protective' oxide growth. *Phil. Trans. R. Soc. Lond. A* 319, 219-247, 1986.
25. L. Martinelli. Mécanismes de corrosion de l'acier T91 par l'eutectique Pb-Bi utilisé comme matériau de spallation. Thèse de doctorat, Université de Paris VI, 2005.
26. J.E. King, P.J. Cotterill. Role of oxides in fatigue crack propagation. *Materials science and technology*, Vol. 6, pp. 19-31, 1990.
27. H. Nakamura, K. Murali, K. Minakawa, A.J. McEvily. Fatigue crack growth in ferritic steels as influenced by elevated temperature and environment. *Microstructure and Mechanical behaviour of materials*, Vol 1, pp 43-57.
28. S.L. Mannan, M. Valsan. High temperature low cycle fatigue of steels and their welds. *Key Engineering Materials* Vols. 274-276 (2004) pp. 57-64.
29. L. Mikulova, F. Schubert. Investigation of creep and creep fatigue crack growth behaviour of P92 in different atmospheres at temperatures above 500°C. ECCC creep conference, Creep & Fracture in high temperature components - Design & life assessment issues. London UK, Destech Publications, Inc. 2005.
30. J. Zurek, E. Wessel, L. Niewolak, F. Schmitz, T.U. Kern, L. Singheiser, W.J. Quadackers. Anomalous Temperature dependence of oxidation kinetics during steam oxidation of ferritic steels in the temperature range 550-650°C. *Corrosion Science* 46, 2301-2317, 2004.
31. R.P. Skelton, J.I. Bucklow. Cyclic oxidation and crack growth during high strain fatigue of low alloy steel. *Metal Science*, 1978.
32. G. Ward, B.S. Hockenhull, P. Hancock. The effect of cyclic stressing on the oxidation of a low-carbon steel. *Metallurgical Transactions*, Vol.5, 1451-1455, 1974.
33. M.S. Hu, A.G. Evans. The cracking and decohesion of thin films on ductile substrates. *Acta metall.* Vol. 37, pp. 917-925, 1989.
34. J. Robertson, M.I. Manning. Limits to adherence of oxide scales. *Materials Science and Technology*. Vol. 6, pp. 81-90, 1990.
35. A.G. Evans, G.B. Crumley, R.E. Demaray. On the mechanical behaviour of brittle coatings and layers. *Oxidation of Metals*, vol. 20, N° 5/6, 1983.
36. H. E. Evans, R. C. Lobb. Conditions for the initiation of oxide-scale cracking and spallation. *Corrosion Science*, Vol. 24, No. 3, pp. 209-222, 1984.
37. M. Schütze. Deformation and cracking behaviour of protective oxide scales on heat-resistant steels under tensile strain. *Oxidation of Metals*, VOL. 24, No. ¾, 1985.
38. J. Barbehön, A. Rahmel, M. Schütze. Behavior of the scale on a 9.5Cr steel under cyclical deformation of the base metal. *Oxidation of Metals*, Vol. 30, Nos. 1/2, 1988.

39. J.C. Grosskreutz. Mechanical properties of metal oxide films. *Journal of Electrochemical Society*, Vol. 116, No. 9, 1969.
40. J. Barbehön, A. Rahmel, M. Schütze. Investigation of the interaction of LCF and oxidation. In *Low cycle fatigue and elasto-plastic behaviour of materials*. Elsevier applied science, 1987.
41. S. Osgerby. Oxide scale damage and spallation in P92 martensitic steel. *Microscopy of oxidation*, 2000.
42. H.E. Evans. Spallation of oxide from stainless steel AGR nuclear fuel cladding : mechanisms and consequences. *Materials Science and Technology*, 4, 415-420, 1988.
43. M. Schütze. Stresses and decohesion of oxide scales. *Materials Science and Technology*, 4, 407-414, 1988.
44. M. Schütze. Mechanical properties of oxide scales. *Oxidation of Metals*, Vol. 44, Nos. 1/2, 1995.
45. R. Vasina, P. Lukas, L. Kunz and V. Sklenicka. Interaction of high cycle fatigue and creep in 9%Cr-1Mo steel at elevated temperature. *Fatigue Fract. Engng Mater. Struct.* Vol. 18, No. 1, pp. 27-35, 1995.
46. T. Gengenbach, A. Klenk. Creep, creep-fatigue crack initiation and growth in 9-12% chromium steels. *OMNI*, Vol.3, 2004.
47. P. Lukas, L. Kunz, V. Sklenicka. Interaction of high cycle fatigue with high temperature creep in two creep-resistant steels. *Mat. Sci. Eng. A129* (1990) 249-255.

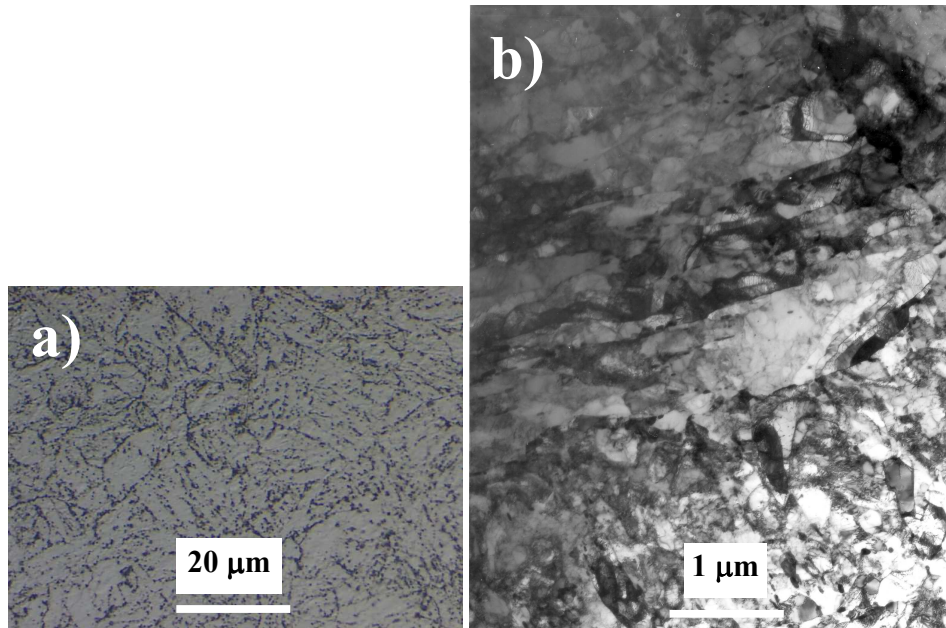


Figure 1 – As-tempered microstructure observed by optical microscopy after etching by Vilella's reagent a) and by TEM b).

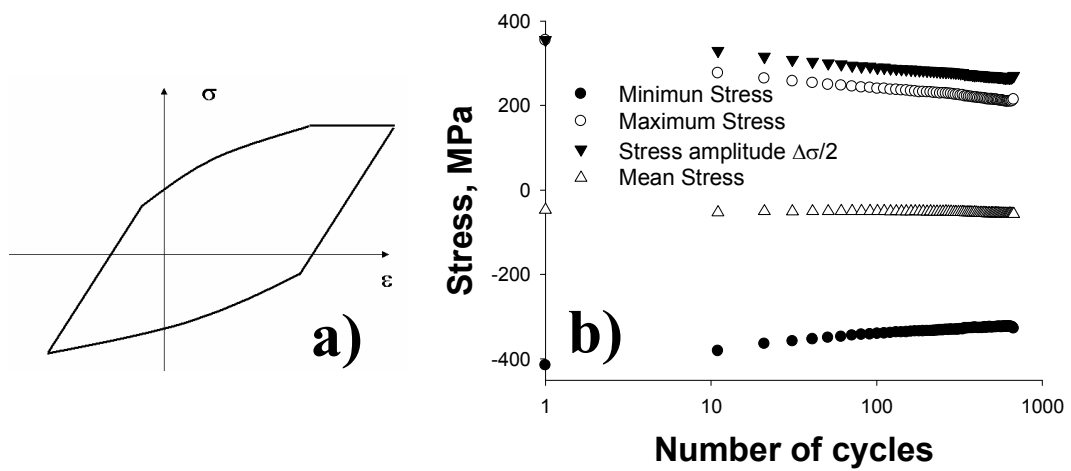


Figure 2 – a) Schematic stress-strain hysteresis loop obtained for a creep fatigue test and b) evolution of the peak stresses, the mean stress and the stress amplitude for a creep-fatigue test held in tension ( $\Delta\epsilon_f=0.7\%$ , hold time : 30min) .

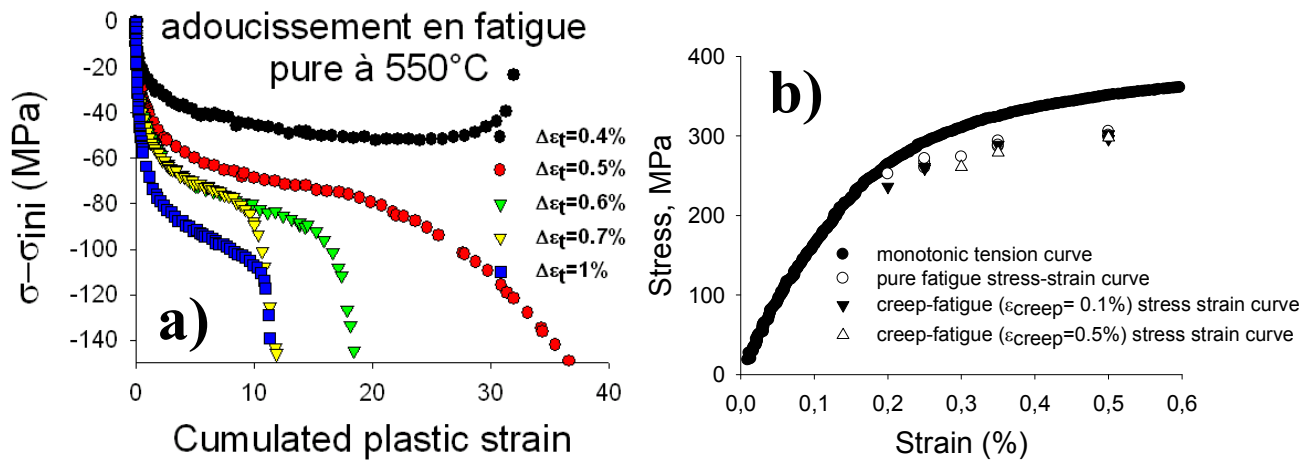


Figure 3 - a) Cyclic softening effect observed under pure fatigue loadings for various strain amplitudes and b) comparison between the monotonic tensile curve and the cyclic stress-strain curve ( $\Delta\sigma/2$  values) obtained at  $N_f/2$ .

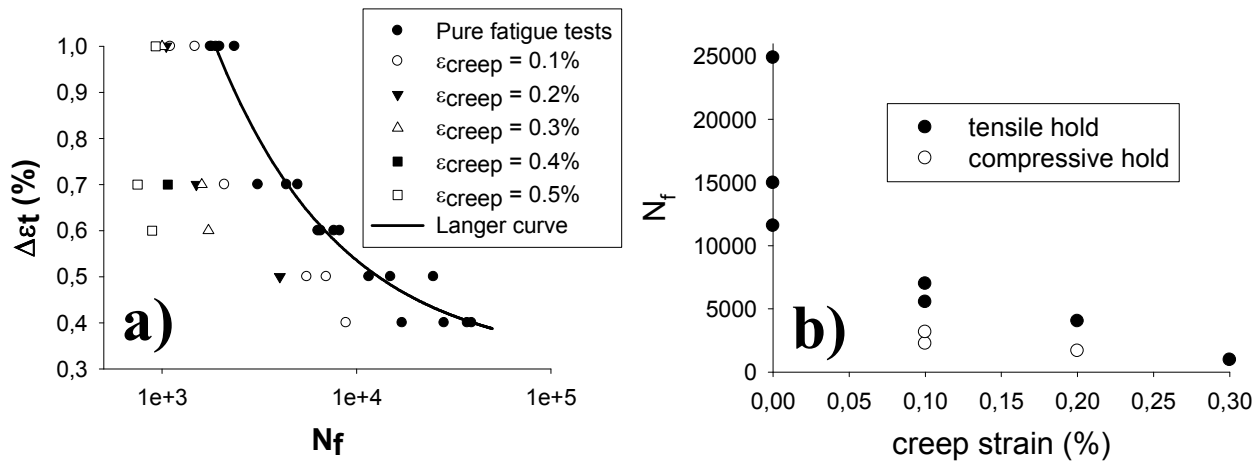


Figure 4 - a) SN-like curve for fatigue and creep fatigue tests at 823K in air and b) deleterious effect of tensile and compressive creep holds ( $\Delta\epsilon_t = 0.5\%$ ).

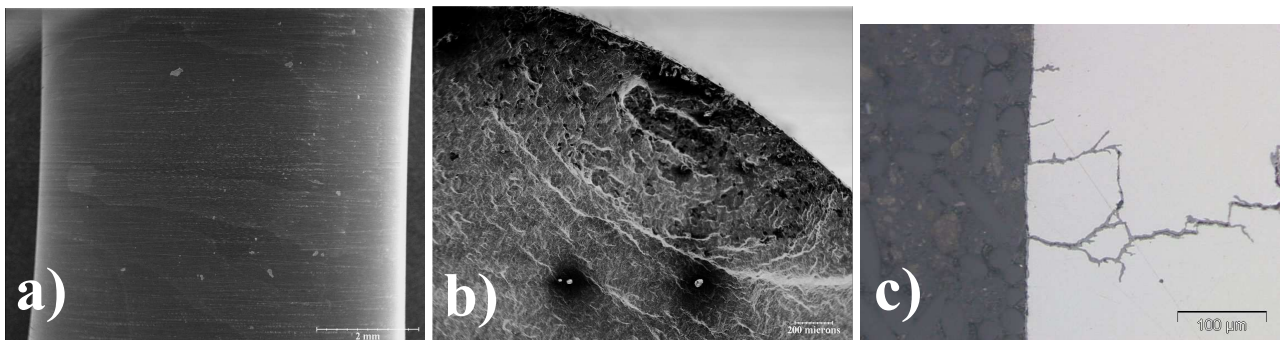


Figure 5 - Observations of a sample tested under pure fatigue loading ( $\Delta\epsilon_t = 0.7\%$ ) a) on the sample surface, b) on the fracture surface, c) on longitudinal cross-section.



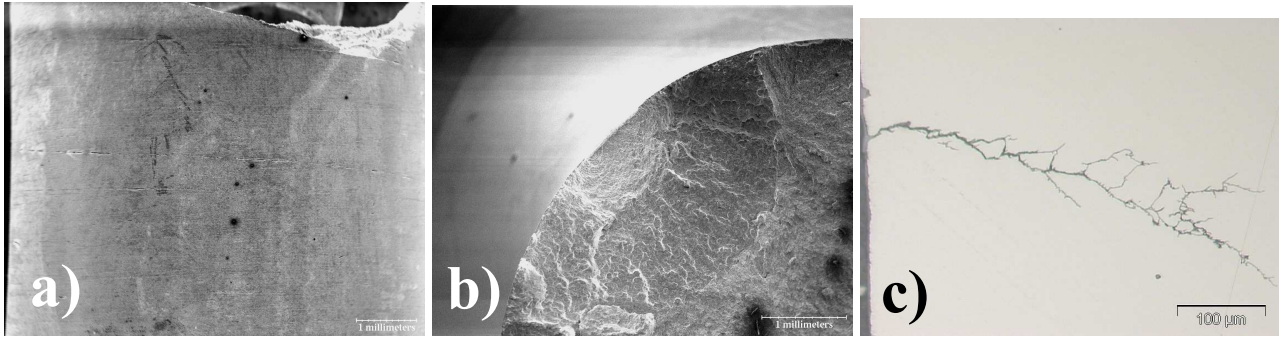


Figure 6 - Observations of a sample tested under creep-fatigue loading with a tensile hold time ( $\Delta\epsilon_t=0.4\%$ ,  $\epsilon_{creep}=0.1\%$ ) a) on the sample surface, b) on the fracture surface, c) on longitudinal cross-section.

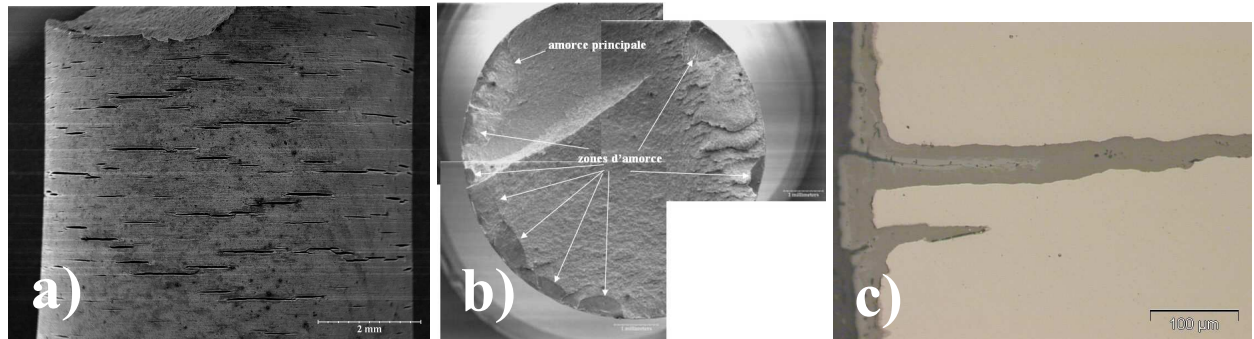


Figure 7 - Observations of a sample tested under creep-fatigue loading with a compressive hold time ( $\Delta\epsilon_t=0.4\%$ ,  $\epsilon_{creep}=0.1\%$ ) a) on the sample surface, b) on the fracture surface, c) on longitudinal cross-section.

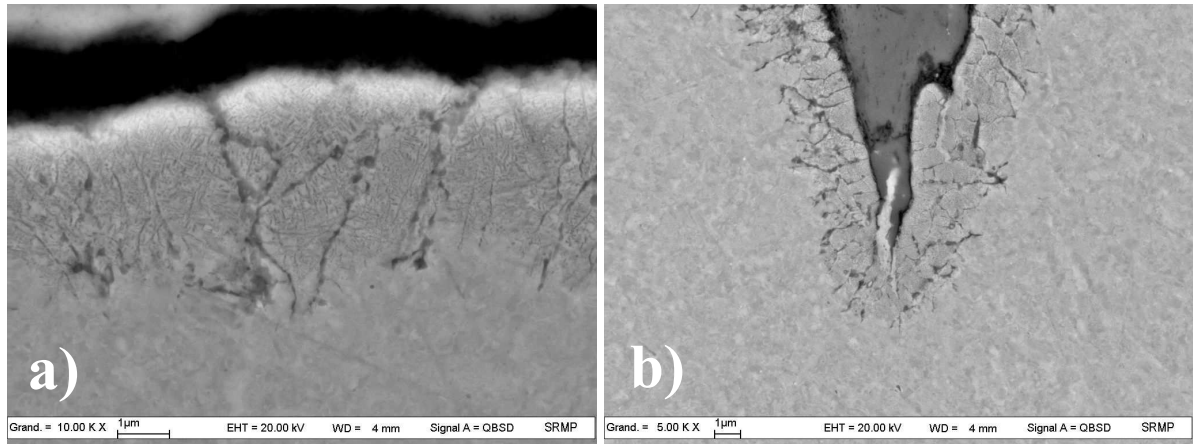


Figure 8 - observations of the internal oxide layer visible a) on the sample surface and b) at the crack tip, when the oxide is not adherent to the substrate.

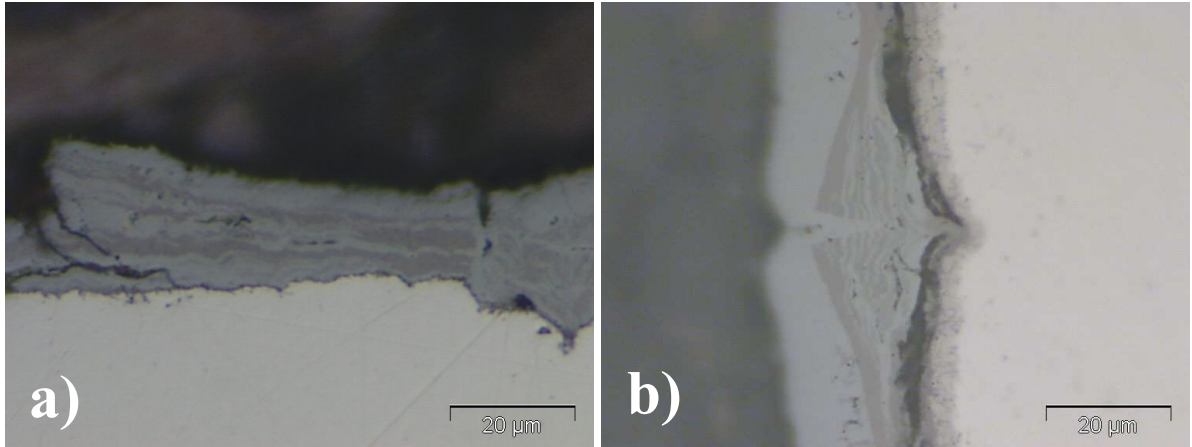


Figure 9 - multilayered oxide observed on a cross-section of the creep fatigue test with a compressive hold period ( $\Delta\epsilon_t=0.4\%$ ,  $\epsilon_{\text{creep}}=0.1\%$ ).

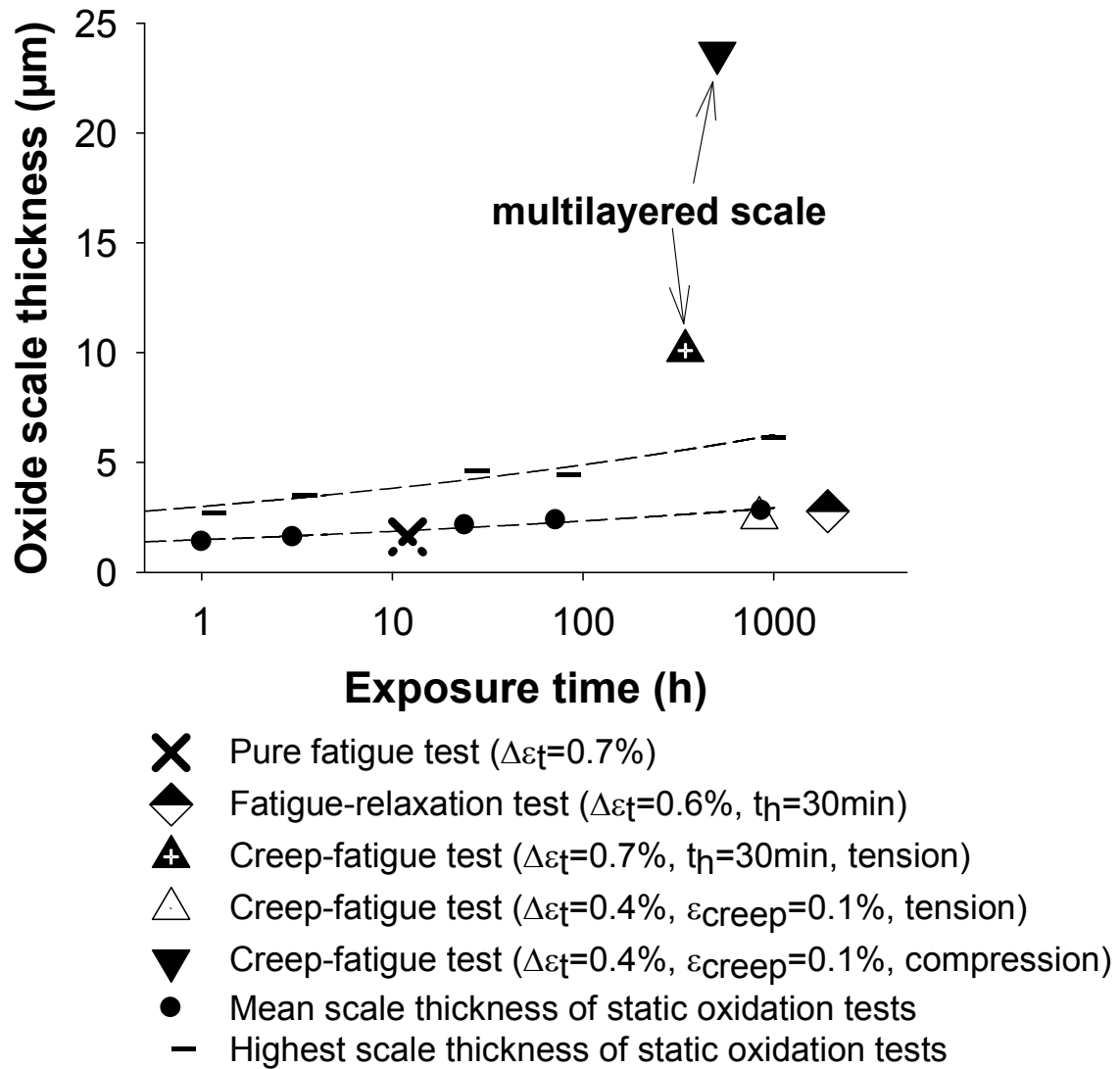


Figure 10 - Thicknesses of the oxide scale measured under static oxidation (823K in air) and after various mechanical tests.

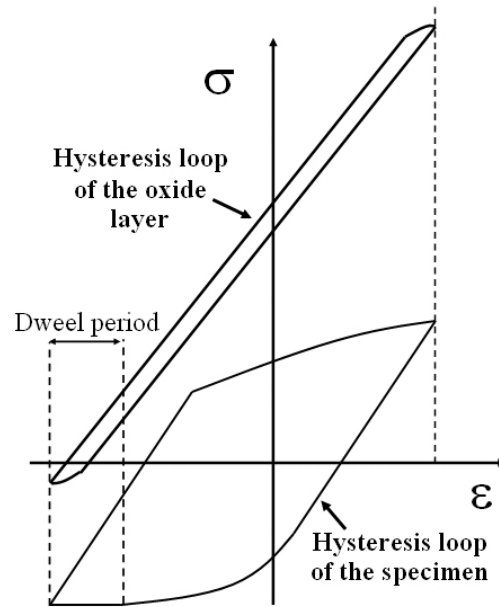


Figure 11 - Schematic representation of the loading cycle experienced by the oxide layer under compressive hold creep fatigue test.